Large magnetoresistance in the antiferromagnetic semimetal NdSb

N. Wakeham,[1] E. D. Bauer,[1] M. Neupane,[2] and F. Ronning[1]

[1]*Los Alamos National Laboratory, Los Alamos, New Mexico 87545, USA*
[2]*Department of Physics, University of Central Florida, Orlando, Florida 32816, USA*

There has been considerable interest in topological semimetals that exhibit extreme magnetoresistance (XMR). These have included materials lacking inversion symmetry such as TaAs, as well Dirac semimetals such as Cd_3As_2. However, it was reported recently that LaSb and LaBi also exhibit XMR, even though the rocksalt structure of these materials has inversion symmetry, and the band-structure calculations do not show a Dirac dispersion in the bulk. Here, we present magnetoresistance and specific-heat measurements on NdSb, which is isostructural with LaSb. NdSb has an antiferromagnetic ground state and, in analogy with the lanthanum monopnictides, is expected to be a topologically nontrivial semimetal. We show that NdSb has an XMR of $\sim 10^4\%$, even within the antiferromagnetic state, illustrating that XMR can occur independently of the absence of time-reversal symmetry breaking in zero magnetic field. The persistence of XMR in a magnetic system offers the promise of new functionality when combining topological matter with electronic correlations. We also find that in an applied magnetic field below the Néel temperature there is a first-order transition, consistent with evidence from previous neutron scattering work.

I. INTRODUCTION

Conventional nonmagnetic metallic systems generally show a small positive magnetoresistance (MR) of a few percent, and this behavior can be well described by Boltzmann transport theory [1]. Recently, there has been a great deal of interest in nonmagnetic topological metals that show an extreme magnetoresistance (XMR) of $\sim 10^5\%$ [2–9]. These XMR materials are all semimetals, with close compensation of electrons and holes and very high carrier mobilities. However, these materials also show some unique features because of the topology of their electronic structures. For example, Cd_3As_2 has a symmetry-protected linearly dispersive band crossing and is therefore designated a Dirac semimetal [2,3]. TaAs breaks inversion symmetry, causing the doubly degenerate Dirac dispersions to split into a pair of Weyl cones [4]. XMR was also recently extended to include lanthanum monopnictides [5–7]. These compounds are also topologically nontrivial, although in a different sense than Weyl or Dirac semimetals [8]. They have a simple rocksalt structure with inversion symmetry, and they do not have accidental linear band crossings near the Fermi energy. Instead, they possess a band inversion, which classifies them as topological in the same vein as topological insulators, even though the bulk bands are semimetallic as opposed to insulating. This has led to suggestions that the XMR in these materials is the result of the applied field breaking time-reversal symmetry (TRS) and destroying the topological protection of the conductive states to electron backscattering [7].

The significance of the TRS makes it interesting to investigate similar semimetal materials with a magnetic ground state. In these systems, TRS will be broken even before the application of a magnetic field, and therefore, one might expect significant backscattering at zero field, in contrast to other XMR semimetals. Also, by adding strong electronic correlations, ubiquitous in f-electron systems, one opens the possibility of discovering completely new states of matter with unprecedented functionality not possible in

noncorrelated matter [10–12]. The interplay of magnetism and the XMR may be a route to new technological functionality in these materials. Here, we report on the resistivity and specific heat of a rare-earth monopnictide, NdSb, which is expected to be a topological semimetal but is known, from magnetic susceptibility [13,14] and neutron scattering measurements [15], to have an antiferromagnetic transition at ~ 15 K. We show NdSb does possess XMR of order $10^4\%$, which is comparable to other topological semimetals [2–9]. We also show that this type-I fcc antiferromagnet has a complex H-T phase diagram at high field, with multiple first-order transitions.

II. EXPERIMENTAL AND COMPUTATIONAL TECHNIQUES

Single crystals of NdSb were grown out of Sn flux [16]. Electrical contacts for resistivity measurements were made on freshly cleaved samples using 25-μm platinum wires spot-welded to the (001) face with current applied in the (100) direction. Specific-heat measurements were performed using the time-relaxation method. In all the measurements discussed here, field was applied in the (001) direction. The temperature was controlled within a Quantum Design physical properties measurement system.

First-principles density functional theory calculations were performed to compute the electronic structure using the WIEN2K code [17]. The Perdew-Burke-Ernzerhof (PBE) functional [18] under the generalized gradient approximation was employed, and spin-orbit coupling was included via a second-order variational scheme. LaSb and NdSb were computed using the rocksalt structure with lattice parameters of $a = 6.499$ and 6.319 Å, respectively [19,20]. As the f moments of Nd are strongly localized, we treated three f electrons on Nd as core electrons.
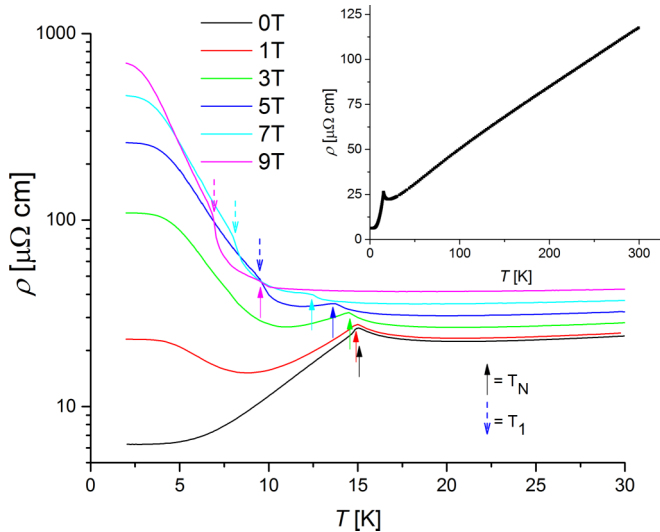
FIG. 1. Resistivity of NdSb as a function temperature at various applied magnetic fields. Solid arrows indicate the Néel temperature T_N; dashed arrows show T_1. Field was applied in the (001) direction perpendicular to the current, which was applied in the (100) direction. The inset shows zero field resistivity up to 300 K.
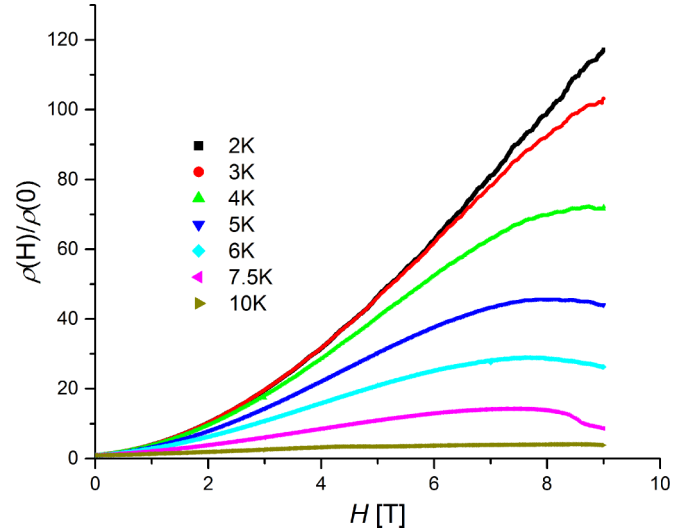

FIG. 2. Magnetoresistance of NdSb as a function of applied magnetic field H at various temperatures. Field was applied in the (001) direction perpendicular to the current, which was applied in the (100) direction.

III. RESULTS AND DISCUSSION

A. Magnetoresistance

Figure 1 shows the resistivity ρ of NdSb as a function of temperature T at several different applied magnetic fields. The inset shows $\rho(T)$ in zero field up to room temperature, which demonstrates a clear peak in the resistivity at the previously reported Néel temperature $T_N = 15$ K [13]. It should be noted that the sensitivity of the resistivity to the magnetic order demonstrates that spin-disorder scattering provides a significant contribution to the total resistivity close to T_N. The absence of a resistive anomaly at 3.7 K (the superconducting transition temperature of Sn) rules out the possible presence of Sn inclusions in our sample.

In an applied magnetic field T_N is suppressed to lower temperature. Above 3 T an additional kink appears in the resistivity significantly below T_N at a temperature we define as T_1. This kink in the resistivity shows that even at finite fields and temperatures well below T_N, there is still a large contribution to the resistivity from spin scattering. In field, at low temperatures the resistivity increases but saturates below 5 K. This behavior is similar to other XMR materials, such as LaBi and LaSb [5–7].

There has yet to be a conclusive explanation of the resistivity upturn in field and the low-temperature saturation in these XMR materials. Evidence has been presented that the large magnetoresistance is the result of the breaking of time-reversal symmetry leading to a loss of topological protection against electron backscattering [2,7]. In such a scenario, the low-temperature saturation is then caused by the electrical shorting effect of conductive topological surface states. However, it has also been argued that in LaBi the large magnetoresistance and resistivity saturation can be explained by a traditional Boltzmann-type two-band model. This type of model is independent of band topology, and the large

magnetoresistance is a consequence of the high mobility of each band and a comparable density of electrons and holes [5,9].

Figure 2 shows the magnetoresistance as a function of field H at several different temperatures. Note the large magnetoresistance of $1.2 \times 10^4\%$ at 2 K and 9 T. This is smaller than reported in some other XMR materials but is comparable to TaAs and Cd_3As_2 when the residual resistivity and the residual resistivity ratio is comparable to our sample [2,4]. We therefore expect even larger magnetoresistance in cleaner rare-earth monopnictide samples. Above 7.5 K there is a clear kink in $\rho(H)$ at high fields. This corresponds to the kink in $\rho(T)$ observed at T_1.

Quantum oscillations can be observed in the MR at low temperatures and high fields. The oscillations were isolated from the nonoscillatory background by subtraction of a seventh-order polynomial fitted to the data. The oscillating contribution to the resistivity $\Delta\rho$ as a function of field is shown at 2 K in Fig. 3(a).

Figure 3(b) shows the amplitude of the fast Fourier transform (FFT) of $\Delta\rho$ at several temperatures as a function of oscillation frequency. The peaks labeled α and β observed at 242 and 397 T, respectively, are likely to correspond to peaks measured at 212 and 433 T in LaSb [7]. We have also labeled the δ, ϵ, and ϕ peaks at lower frequencies as listed in Table I. The suppression of the FFT amplitude of the α, δ, and ϵ peaks is clearly resolved with increasing temperature and is plotted in the inset to Fig. 3(b). These data have been fitted to the Lifshitz-Kosevich formula, and an effective mass has been extracted. We find $m_\alpha^* = 0.25m_e, m_\delta^* = 0.31m_e$, and $m_\epsilon^* = 0.22m_e$. The mass extracted from the α peak is in reasonably close agreement with that reported for LaSb ($0.22m_e$) [6] and LaBi($0.22m_e - 0.35m_e$) [5,6].

In order to investigate the origin of the observed oscillation frequencies we have calculated the Fermi surface (FS) of NdSb and LaSb using density functional theory. The
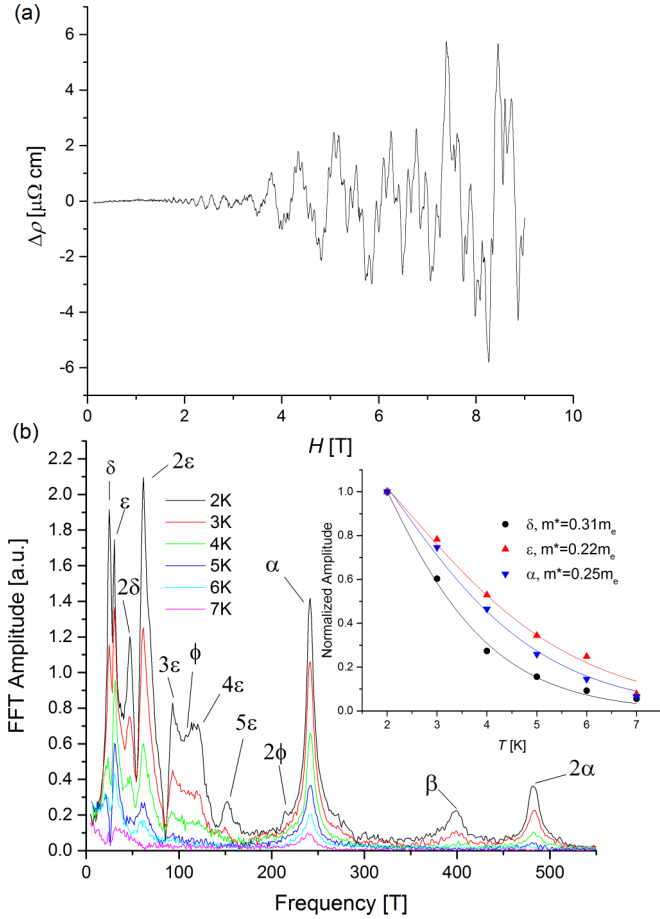
FIG. 3. (a) Oscillatory part of the resistivity $\Delta\rho$ as a function of magnetic field H measured at 2 K. (b) Fast Fourier transform of measured quantum oscillations for various temperatures. The fundamental and harmonic peaks have been identified. The points in the inset show the measured FFT amplitude, normalized at 2K, as a function of temperature for three different orbits. The lines are fits to the Lifshitz-Kosevich formula, and the quoted masses are calculated from the parameters of this fit.
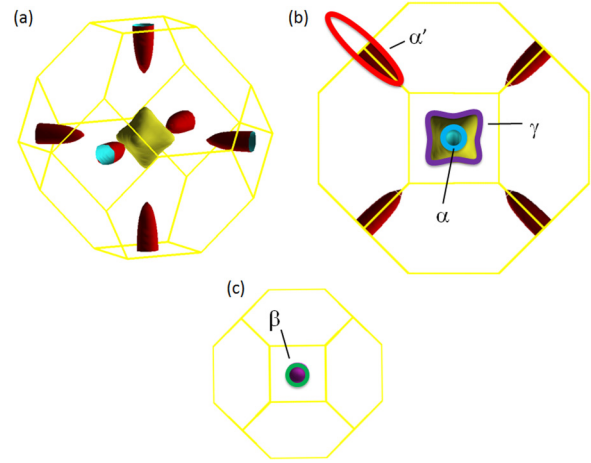

FIG. 4. (a) Calculated Fermi surface of NdSb. (b) Projection of FS perpendicular to the (001) direction. (c) Same projection as in (b), now only showing the central FS pocket. Solid colored lines in (b) and (c) show orbits of different quantum oscillation frequencies. Blue = α orbit, red = α' orbit, green = β orbit, purple = γ orbit.

calculated FS of NdSb in the paramagnetic state is shown in Fig. 4. The projection perpendicular to the (001) direction is shown in Figs. 4(b) and 4(c). There are two hole pockets centered at the Γ point. The smaller spherical hole pocket, shown in Fig. 4(c), is enveloped by the larger yellow octahedral-like pocket in Figs. 4(a) and 4(b). Finally, an electron pocket forms an ellipsoidal Fermi surface which intersects the Brillouin

zone near the $(\pi,0,0)$ point and five other high-symmetry points related by the cubic symmetry. The electronic structure close to the Fermi energy in NdSb is almost identical to both the calculated and measured Fermi surfaces of LaSb [21,22]. For a magnetic field applied along (001) as we have done, four frequencies are expected, as labeled in Figs. 4(b) and 4(c). In LaSb, de Haas–van Alphen (dHvA) measurements have been able to resolve all four extremal orbits [21], while Shubnikov–de Haas (SdH) measurements [7] only observe the smaller two frequencies. Hence, we are not surprised that we also only observe the α and β orbits in our SdH measurements. We find reasonable agreement between the calculated and observed frequencies for the α and β orbits. However, we do note that the agreement is not as good for NdSb as for LaSb. This difference may be related to a small tetragonal distortion, which occurs upon entering the magnetically ordered state [23] and/or the influence of the Nd magnetism on the electronic structure.

Note that without including long-range magnetic order there is no way to account for the proliferation of observed frequencies below 200 T. At least three unique frequencies labeled δ, ϵ, and ϕ can be identified. The additional peaks can be assigned to harmonics of these three frequencies, although they may also contain additional orbits as well. The origin of these additional frequencies not observed in the La analogs is a natural consequence of the Brillouin zone folding, which occurs due to the long-range antiferromagnetic order. Confirmation of this would require data to higher fields in order to separate the frequencies present above and below $T_N(H)$.

B. Antiferromagnetism

NdSb is a type-I fcc antiferromagnet with ferromagnetically aligned planes of Nd moments, antiferromagnetically coupled in the (001) direction. The moments are aligned in the (001) direction [15]. The antiferromagnetic transition can clearly be seen as a peak in the specific heat divided by temperature

TABLE I. Quantum oscillation frequencies of experimental SdH and dHvA measurements and theoretical orbits for LaSb and NdSb. Frequencies are in teslas.

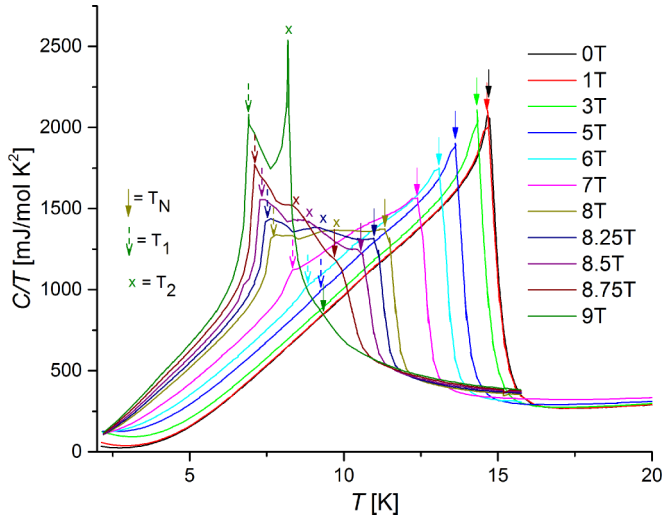|	Orbit	α	α'	β	γ	δ	ϵ	ϕ
LaSb	Expt. (dHvA) [21]	236	923	480	1189			
	Expt. (SdH) [6]	212		433				
	Theory	224	1008	480	1332			
NdSb	Expt. (SdH)	242		397		24	30	107
	Theory	296	1380	736	1728			

FIG. 5. Specific heat C divided by temperature T of NdSb as a function of T at various applied magnetic fields. Solid arrows indicate the Néel temperature T_N, dashed arrows show T_1, and crosses indicate T_2. Field was applied in the (001) direction.

FIG. 6. Phase diagram of NdSb as a function of field and temperature, taken from our measurements of resistivity ρ and specific heat C, as well as previous neutron scattering measurements N [25].

C/T as a function of temperature, shown in Fig. 5. The magnetic entropy up to T_N estimated from these data is $0.85R\ln(4)$, where R is the universal gas constant. This is in good agreement with that expected for this system, where the f electrons of Nd are localized, and the ground state of the system is a quartet [15,24]. This model of a localized moment is also consistent with the observation that the ordered moment in NdSb is very close to the free-ion value [15]. These observations justify the treatment of the Nd moments as localized in our FS calculations.

In a magnetic field applied in the (001) direction T_N decreases with increasing field, as expected. In addition, at fields above 5 T there is a second feature in C/T below T_N marked by a dashed arrow in Fig. 5. For example, at 7 T there is a kink in C/T at around 8.3 K. This coincides with the kink seen in the resistivity shown in Fig. 1 at T_1. As the field is increased further to 9 T, the kink in C/T becomes a peak at 7 K, and the transition becomes strongly first order. The antiferromagnetic transition becomes less pronounced at high fields and is only a very small kink at 9.8 K at 9 T. There is also a third feature in C/T at a temperature between T_N and T_1 marked by crosses that we define as T_2. This feature becomes very well defined and first order at 9 T at 8.2 K. No feature of this transition was observed in resistivity measurements.

Figure 6 shows the magnetic phase diagram constructed from the resistivity and specific-heat measurements of NdSb. There are multiple possible explanations for the complexities of the H-T phase diagram. From the symmetry of the antiferromagnetic (AFM) order, in zero field one would expect equal populations of magnetic domains with the AFM Q vector along the (100), (010), and (001) directions. However, it was shown from neutron scattering measurements that in NdSb this is not the case. In fact, the population of each domain is different in zero field, and the (001) domain fraction is dominant near T_N when field is applied in the (001) direction [25]. Furthermore, in sufficiently high field, as temperature is reduced, the population of the (001) domain is
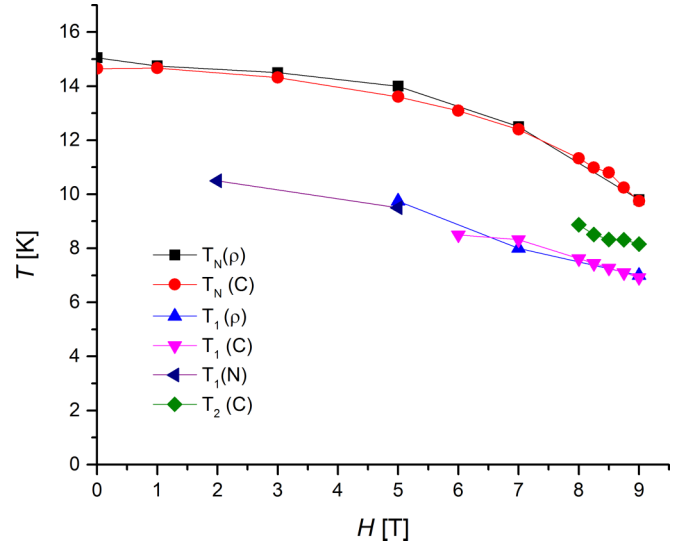
suddenly quenched, and the populations of the (100) and (010) domains are enhanced. The temperature of this first-order transition has been added to our H-T phase diagram in Fig. 6. This phase boundary coincides perfectly with the anomalies we observe in resistivity and heat capacity and have labeled as T_1. The transition observed at T_2 could be the result of an intermediate domain population distribution between that at zero field and T_1. However, in this scenario it is difficult to understand why this would not produce a feature in the resistivity when the transition at T_1 clearly does. Therefore, we consider that the transition at T_2 may have a different origin than that at T_1. This could be a reorientation of spins within a domain, such as a spin-flop transition. Other than magnetic domain redistribution, it was also suggested that the phase transition at T_1 could involve multi-Q ordering [26]. Hence, it is possible that the phase transition at T_2 involves another magnetically ordered state. Additional microscopic measurements in high magnetic fields could help identify which of these scenarios occurs. Finally, we note that the first excited crystal field level in NdSb is only 1.2 meV above the ground-state energy [27] and hence will play a role in determining the subtleties of the phase diagram.

IV. CONCLUSION

In conclusion, through measurements of the resistivity and specific heat we have shown that the antiferromagnetic topological semimetal NdSb has a complex H-T phase diagram. Transport measurements also show XMR that is qualitatively and quantitatively consistent with that observed in the nonmagnetic lanthanum monopnictide analogs, LaSb and LaBi. This suggests that the large magnetoresistance is not solely the result of breaking TRS on a topological conductive state. Quantum oscillation measurements demonstrate that the FS of NdSb is similar to that of LaSb, although with the

addition of lower-frequency peaks, which we attribute to zone folding because of the magnetic ground state. In addition, the transport is sensitive to the spin-disorder scattering, which occurs most notably near T_N. The persistence of XMR in NdSb, despite the clear influence of magnetism on the resistivity, emphasizes that magnetism can coexist with the high mobilities often found in topological materials.

[1] N. Mermin and N. Ashcroft, *Solid State Physics* (Saunders College, Philadelphia, PA, 1976).

[2] T. Liang, Q. Gibson, M. N. Ali, M. Liu, R. J. Cava, and N. P. Ong, Nat. Mater. **14**, 280 (2014).

[3] M. Neupane, S.-Y. Xu, R. Sankar, N. Alidoust, G. Bian, C. Liu, I. Belopolski, T.-R. Chang, H.-T. Jeng, H. Lin, A. Bansil, F. Chou, and M. Z. Hasan, Nat. Commun. **5**, 3786 (2014).

[4] L. X. Yang, Z. K. Liu, Y. Sun, H. Peng, H. F. Yang, T. Zhang, B. Zhou, Y. Zhang, Y. F. Guo, M. Rahn, D. Prabhakaran, Z. Hussain, S.-K. Mo, C. Felser, B. Yan, and Y. L. Chen, Nat. Phys. **11**, 728 (2015).

[5] S. Sun, Q. Wang, P.-J. Guo, K. Liu, and H. Lei, arXiv:1601.04618.

[6] F. F. Tafti, Q. D. Gibson, S. K. Kushwaha, J. W. Krizan, N. Haldolaarachchige, and R. J. Cava, arXiv:1602.01525.

[7] F. F. Tafti, Q. D. Gibson, S. K. Kushwaha, N. Haldolaarachchige, and R. J. Cava, Nat. Phys. **12**, 272 (2016).

[8] M. Zeng, C. Fang, G. Chang, Y.-A. Chen, T. Hsieh, A. Bansil, H. Lin, and L. Fu, arXiv:1504.03492.

[9] M. N. Ali, J. Xiong, S. Flynn, J. Tao, Q. D. Gibson, L. M. Schoop, T. Liang, N. Haldolaarachchige, M. Hirschberger, N. P. Ong, and R. J. Cava, Nature **514**, 205 (2014).

[10] M. Dzero, K. Sun, V. Galitski, and P. Coleman, Phys. Rev. Lett. **104**, 106408 (2010).

[11] M. Hohenadler and F. F. Assaad, J. Phys. Condens. Matter **25**, 143201 (2013).

[12] E. Tang, J.-W. Mei, and X.-G. Wen, Phys. Rev. Lett. **106**, 236802 (2011).

[13] G. Busch, O. Marinček, A. Menth, and O. Vogt, Phys. Lett. **14**, 262 (1965).

[14] T. Tsuchida, Y. Nakamura, and T. Kaneko, J. Phys. Soc. Jpn. **26**, 284 (1969).

[15] P. Schobinger-Papamantellos, P. Fischer, O. Vogt, and E. Kaldis, J. Phys. C **6**, 725 (1973).

[16] P. C. Canfield and Z. Fisk, Philos. Mag., Part B **65**, 1117 (1992).

[17] J. Blaha, P. Schwarz, K. Madsen, G. K. H. Kvasnicka, and D. Luitz, WIEN2K, *An Augmented Plane Wave+Local Orbitals Program for Calculating Crystal Properties* (Vienna University of Technology, Vienna, 2001).

[18] J. P. Perdew, K. Burke, and M. Ernzerhof, Phys. Rev. Lett. **77**, 3865 (1996).

[19] G. V. Samsonov, M. N. Abdusalyamova, Kh. Shokirov, and S. A. Pryakhina, Izv. Akad. Nauk SSSR Neorg. Mater. **10**, 1951 (1974) [Inorg. Mater. **10**, 1672 (1974)].

[20] M. Abdusalyamova, H. Shokirov, and O. Rakhmatov, J. Less Common Met. **166**, 221 (1990).

[21] H. Kitazawa, T. Suzuki, M. Sera, I. Oguro, A. Yanase, A. Hasegawa, and T. Kasuya, J. Magn. Magn. Mater. **31–34**, 421 (1983).

[22] A. Hasegawa, J. Phys. Soc. Jpn. **54**, 677 (1985).

[23] F. Lévy, Phys. Kondens. Mater. **10**, 85 (1969).

[24] A. Furrer, W. J. L. Buyers, R. M. Nicklow, and O. Vogt, Phys. Rev. B **14**, 179 (1976).

[25] D. Mukamel, J. M. Hastings, L. M. Corliss, and J. Zhuang, Phys. Rev. B **32**, 7367 (1985).

[26] O. Vogt and K. Mattenberger, *Handbook on the Physics and Chemistry of Rare Earths*, Vol. 17 (Elsevier Science, New York, 1993).

[27] A. Furrer, J. Kjems, and O. Vogt, J. Phys. C **5**, 2246 (1972).